International Journal of Heat and Fluid Flow 30 (2009) 741–750

Contents lists available at ScienceDirect

International Journal of Heat and Fluid Flow

journal homepage: www.elsevier.com/locate/ijhff

Simulations of free surface flows with implementation of surface tension and interface sharpening in the two-fluid model

L. Štrubelj [a], I. Tiselj [a,*], B. Mavko [b]

[a] Jožef Stefan Institute, Reactor Engineering Division (R4), Jamova cesta 39, 1000 Ljubljana, Slovenia
[b] Faculty of Mathematics and Physics, University of Ljubljana, Jadranska ulica 19, 1000, Ljubljana, Slovenia

ARTICLE INFO

Article history:
Received 28 November 2008
Received in revised form 10 February 2009
Accepted 23 February 2009
Available online 29 March 2009

Keywords:
Free surface flow
Two-fluid model
Interface sharpening
Computational multi-fluid dynamics
Surface tension

ABSTRACT

Two-fluid model used for free surface flows with large characteristic scales is improved; the smeared interface is sharpened with conservative level set method and the surface tension force with wetting angle is implemented. Surface tension force is split between two phases with several models. Detailed analysis showed the splitting of surface tension force with volume averaging as the most appropriate. The improved two-fluid model with interface sharpening and implemented surface tension is validated on several test cases. The pressure jump over a droplet interface test case showed that the pressure jump in simulation converges with grid refinement to the analytical one. The parasitic currents in simulation are one order of magnitude larger than in simulation with volume of fluid model. In the oscillating droplet test case the time period of oscillating droplet with initially ellipsoid or square shape is similar to the analytical time period. In the rising bubble test case, the rising bubble position, terminal velocity, and circularity are similar to the one observed in simulations with level set model. The wetting angle is implemented in the two-fluid model with interface sharpening and surface tension force. Model is tested in the simulation of droplet in contact with wall with different wetting angles.

1. Introduction

Two-phase flows are flows of two immiscible fluids separated by the interface and appear in several industrial applications (nuclear power plants, other power systems, heat transfer systems, process systems, transport systems, etc.), biological systems (cardiovascular system, respiratory system, etc.) and natural phenomena (ocean waves, river flooding, etc.).

Topological classification of the two-phase flows is based on interface structures. Two-phase flows can be divided in three major groups and several subgroups – flow regimes:

- Stratified flows (film flow, annular flow, horizontal stratified and jet flow)
- Mixed or transitional flows (cap, slug, churn-turbulent flow, bubbly annular flow, droplet annular flow and bubbly droplet annular flow)
- Dispersed flows (bubbly flow, droplet flow and flow with solid particles)

The upper classification of subgroups (flow regimes) is convenient for flows in the pipes, which are predominantly one-dimensional and were historically simulated with one-dimensional two-fluid models, such as implemented in the system codes RELAP (The RELAP5 Code, 1995), CATHARE (Bestion, 1990) or WAHA (Tiselj et al., 2004). In 2D or 3D the classification into three major groups is more convenient. Stratified flows are flows where large interfaces are present and dispersed flows are flows with many small droplets, bubbles or particles. A natural criteria to determine whether the flow is stratified or dispersed is our ability to resolve the interface: in experiments or in simulations. In two-phase flow simulations, grid spacing can play a similar role as in the LES models of turbulent flows: sufficiently large interfaces can be resolved on a given grid, while too small characteristic dimensions of the dispersed flow surface represent sub-grid structures that must be modeled with appropriate models. Mixed two-phase flows are dispersed in one and stratified in the other region of the flow domain.

The expression "free surface flow" used in the present paper, is often replaced with expression "stratified two-phase flow", sometimes also "flow with deformable interface" or "separated flow" in the literature (Crowe, 2005).

Various multi-dimensional numerical models were developed to simulate stratified flows: Marker and Cell (Harlow and Welch, 1965), Lagrangian grid methods (Hirt et al., 1974; Hyman, 1984), volume of fluid method (Hirt and Nichols, 1981), level set method (Osher and Sethian, 1988; Sussman, 1994) and Front-Tracking method (Tryggvason et al., 2001). These methods are able to accurately capture the physics of the stratified flows. On the other side,

* Corresponding author. Tel.: +386 15885330; fax: +386 15885377.
E-mail addresses: luka.strubelj@ijs.si (L. Štrubelj), iztok.tiselj@ijs.si (I. Tiselj), borut.mavko@ijs.si (B. Mavko).

0142-727X/$ - see front matter © 2009 Elsevier Inc. All rights reserved.
doi:10.1016/j.ijheatfluidflow.2009.02.009

Nomenclature

Latin letters

c_D	drag coefficient
C	circularity
d	interfacial length scale [m]
Eo	Eötvös number
H	height [m]
$\vec{n}$	normal to the interface
$\vec{n}_{wall}$	normal to the wall
m	mass [kg]
n	oscillation mode
p	pressure [Pa]
P	perimeter [m]
r	radius [m]
Re	Reynolds number
t	time [s]
$\vec{t}$	tangent
$\vec{u}$	velocity vector
u	velocity in x direction [m/s]
v	velocity in y direction [m/s]
V	volume [m^3]

Greek letters

α	volume fraction
β	splitting factor of surface tension force
Δx	grid spacing in x direction [m]
Δy	grid spacing in y direction [m]
Δt	timestep [s]
$\Delta\tau$	artificial timestep used in conservative level set method
ε	artificial viscosity in conservative level set method
Θ	wetting angle [°]
κ	curvature [m^{-2}]
μ	dynamic viscosity [Pa s]
π	number pi
ρ	density [kg/m^3]
σ	surface tension [N/m]
τ	artificial time in conservative level set method, oscillation time period [s]
ω	oscillation frequency [s^{-1}]

Subscripts

1	corresponds to fluid 1
2	corresponds to fluid 2
0	initial
d	drag
k	property of fluid k
m	mixture
wall	at the wall

Superscripts

$'$	pressure correction
$*$	intermediate
n	nth timestep

two-fluid models (also called interpenetrating continuum models) have been successfully applied for simulations of rather complex dispersed flows (Končar and Krepper, 2008). Probably the biggest challenge in the two-phase flow modeling are the so-called mixed flows where dispersed and stratified flows are observed in the same flow domain. Such flows are commonly present in nature (wave breaking) and industry (condensation induced water hammer – (Prasser et al., 2004)). One of the first attempts to simulate mixed flows was presented by Černe et al. (2001) who coupled the VOF method with the two-fluid model. The main problem of such coupling turned out to be coupling of two rather different mathematical models with different number of equations in the same computational domain.

An attempt towards the improved simulations of the mixed two-phase flows is described in the present paper. From the mathematical point of view it is the most convenient to use two-fluid model equations within the whole computational domain and to implement an additional interface tracking/sharpening algorithm within the two-fluid model, when stratified flow is encountered. Such combined model is suitable for both free surface and dispersed flow simulations and can capture the interface position. There are actually three different sub-models required for such approach: the first is an interface tracking/sharpening algorithm that can work within the equations of the two-fluid model. This problem was considered by Štrubelj and Tiselj (submitted for publication) where various flows with interface breakup were simulated. The second required sub-model is needed to take into account surface tension force in two momentum equations of two-fluid model and is a topic of the present paper. The key question in implementation of the surface tension force addressed in the present work considers various possible implementations of the surface tension force in the momentum equations of the two-fluids. The third sub-model is needed in the form of criteria that will determine whether the flow is closer to dispersed or stratified form, i.e., whether to switch on or off the interface tracking algorithm. Criteria for transition between stratified and dispersed flow was proposed by Černe (2001) and is based on errors of the VOF model (Černe et al., 2002); nevertheless, it is believed that importance of this sub-model will require further research in this direction and will present some kind of a basic "flow regime map" for the 3D two-fluid model.

The idea of surface tracking within the two-fluid model is not new. Various two-fluid models have been used for simulations of free surface flows, especially for turbulent free surface flows where turbulence is not resolved, but rather modeled with turbulence model for each phase (Yao et al., 2005). Most of the interface tracking schemes are based on solution of transport equation for the volume of particular fluid (VOF method). An example of this approach can be found in the work of Minato et al. (2000), Nagayoshi et al. (2003). Similar type of interface tracking is implemented in the computer code CFX (ANSYS, 2007) and has been used for modeling of horizontally stratified pipe flows by Vallée et al. (2005), Frank (2005), Höhne et al. (2007), Wintterle et al. (2008), Scheuerer et al. (2007). Bartosiewicz et al. (2008), Coste et al. (2007) used two-fluid approach with advection of volume fraction, implemented in the Neptune_CFD code.

The first attempt to implement surface tension in the two-fluid model was presented by Bartosiewicz et al. (2008). The surface tension force was computed as a volume force as proposed by Brackbill (1992). The surface tension force was split between two phases, i.e. between two momentum equations with splitting factors, which sum must be equal to 1. Two approaches for splitting factors have been proposed, the first based on local volume averaging and the second based on local mass averaging. Bartosiewicz et al. (2008) concluded that both approaches give similar results.

Both models for splitting factors: mass and volume averaging are tested in systems with large density differences in the present paper. Beside the two types of splitting proposed by Bartosiewicz

et al. (2008), some other models were tested: the model where the surface tension force is added only to momentum equation of gas or liquid and another one with unusual splitting factors. All models were tested on numerical test case where pressure jump over a cylindrical droplet interface is calculated. The best and the most correct model for splitting factors, based on minimum error in pressure jump and minimum parasitic velocities is model based on volume averaging. The model where surface tension force is implemented only to lighter phase has also shown very good results. We have shown that the convergence with grid refinement is different for used models. In further simulations we used model for splitting factor based on volume averaging. The droplet oscillating time period, rising bubble position, velocity, volume conservation and circularity were analyzed. We have also demonstrated that droplet in contact with wall with different wetting angles can be simulated with two-fluid model with interface sharpening and surface tension force.

2. Physical models

In this section, the applied two-fluid model, implemented in an "in-house" code is described. The equations of incompressible and isothermal two-fluid model are considered. Detailed derivation of the two-fluid model can be found in the book of Ishii and Hibiki (2006). Two-fluid model follows from the spatial, temporal or ensemble averaging of the Navier–Stokes equations. The main purpose of such averaging is similar to the Reynolds averaging of the single-phase Navier–Stokes equations of turbulent flows: to avoid description of the very small scales that may appear in the two-phase flow. Such averaging is a mandatory procedure when one aims to simulate two-phase flows with complex and rapidly changing topology of the interfacial surface. The balance equations of the incompressible, isothermal two-fluid model can be written as two pairs of mass and momentum balances:

$$\frac{\partial \alpha_k}{\partial t} + \vec{u}_k \cdot \nabla \alpha_k = 0 \tag{1}$$

$$\frac{\partial (\rho_k \alpha_k \vec{u}_k)}{\partial t} + (\rho_k \alpha_k \vec{u}_k \cdot \nabla)\vec{u}_k = -\alpha_k \nabla p + \nabla \cdot (\mu_k \alpha_k \nabla \vec{u}_k) + \rho_k \alpha_k \vec{g} + \vec{F}_{D,k} + \vec{F}_{S,k} \tag{2}$$

where index k denotes fluid 1 or 2 and α_k denotes volume fraction of the particular phase and $\vec{u}_k$ velocity in the given point. Two interfacial forces: drag force $\vec{F}_{D,k}$ and surface tension force $\vec{F}_{S,k}$ acts between phases. Volume fractions of both fluids are related with simple relations $\alpha_1 + \alpha_2 = 1$. The crucial difference between these equations and the single-fluid Navier–Stokes equations used for the two-phase flow simulations is in the fact that two interpenetrating fluids are seen by the two-fluid model and single-fluid with variable properties by the single-fluid model. The latter method must include an interface tracking algorithm in order to describe temporal development of the interfacial surface as an integral part of the solution. Thus, we are discussing two fundamentally different physical pictures: when one is using Navier–Stokes equations supplemented with interface tracking method to describe two-phase flow, only one fluid is present at a given time in the particular point of the domain. When the same two-phase flow is described with the two-fluid model – both phases are assumed to be present in the whole domain at all times with continuously changing ratio of both phases. Velocities of both fluids can be different in the same point of domain.

Despite such a crucial difference between the physical pictures of both types of two-phase flow description, one can notice, that with some additional work, both types of mathematical models can be very similar, which means that it might be possible to merge both approaches within the same simulation of the "mixed" two-phase flow, where the stratified flow and dispersed flow can be found in the same computational domain.

Due to the averaging, additional term $\vec{F}_{D,k}$ appears in momentum equations describing the drag force. The sum of local drag forces of both phases is equal to zero: $\vec{F}_{D,2} = -\vec{F}_{D,1}$. In dispersed flow various types of interfacial forces are implemented, but for free surface flow only drag force ($\vec{F}_{D,k}$) is needed as shown by Štrubelj and Tiselj (submitted for publication). The drag force depends on relative velocity $\vec{u}_2 - \vec{u}_1$, mixture density ρ_m, drag coefficient c_D and interfacial length scale d (Frank, 2005):

$$\vec{F}_{D,1} = \alpha_1 \alpha_2 (\vec{u}_2 - \vec{u}_1)\rho_m \frac{c_D}{d} \tag{3}$$

$$\rho_m = \alpha_1 \rho_1 + \alpha_2 \rho_2 \tag{4}$$

In dispersed flow modeling the interfacial length scale is imposed by the physics of the flow and is equal to bubble/droplet diameter. The drag coefficient is usually a drag coefficient of the sphere with the simplest choice $c_D = 0.44$ Frank, 2005 used in the present work, or a simple function of bubble/droplet Reynolds number $c_D = c_D(Re_{particle})$. The proposed drag force (3) is tested on laminar flows, for turbulent flows the local turbulent parameters should be implemented in the drag force.

In simulations of free surface flows (3) does not represent a realistic physical model. It is reasonable to expect that the velocities of both fluids in the vicinity of the interface are rather similar. Thus, the main purpose of the interfacial drag is to more or less equalize velocities of both fluids at the interface. This can be achieved with any type of the correlation even if such correlation does not have a physical background. This rather simple fact has been demonstrated in various simulations, where the results of the simulations in various stratified flows with two-fluid models (two-fluid velocities) were more or less the same as the results obtained with "homogeneous" two-phase flow model, which assumes that fluid velocities are equal (Štrubelj and Tiselj, submitted for publication). To achieve sufficiently high interphase drag in our simulations, the interfacial length scale was chosen as very small.

For turbulent flows the same interfacial drag closure law can be used if all turbulent scales are simulated. If that is not the case different interfacial drag closure law can give better results. Coste et al. (2008) has developed a model where the drag force is calculated similar as wall friction force (log layer velocity profile: $u^+ = f(y^+)$) in the direction parallel to the interface and as droplet drag force in the direction perpendicular to the interface.

2.1. Implementation of surface tension force

The surface tension force $\vec{F}_S$ is calculated as continuum surface force, based on curvature κ as proposed by Brackbill (1992):

$$\vec{F}_S = \sigma \kappa \nabla \alpha_1 \tag{5}$$

The interface normal $\vec{n}$ is calculated using volume fraction gradients and the curvature κ is calculated using gradients of the interface normal

$$\kappa = -\nabla \cdot \vec{n}, \quad \vec{n} = \frac{\nabla \alpha_1}{|\nabla \alpha_1|} \tag{6}$$

When Brackbill's model is implemented within the two-fluid model, surface tension force is split between two phases occupying the cell, since two momentum equations are solved in our system

$$\vec{F}_{S,k} = \beta_k \vec{F}_S \tag{7}$$

When kinetic equilibrium is assumed the pressure gradient within the two-fluid model is calculated by sum of both momentum equations:

$$(\alpha_1+\alpha_2)\nabla p=(\beta_1+\beta_2)\vec{F}_S \tag{8}$$

The pressure gradient in the two-fluid model should be the same as the pressure gradient in the single-fluid (homogeneous) model $\nabla p=\vec{F}_S$, thus the sum of both averaged factors is unity:

$$\beta_1+\beta_2=1 \tag{9}$$

Bartosiewicz et al. (2008) proposed two models for averaged factor β_k: the first based on mass average:

$$\beta_k=\alpha_k\rho_k/(\alpha_1\rho_1+\alpha_2\rho_2) \tag{10}$$

and second based on volume average in the cell:

$$\beta_k=\alpha_k \tag{11}$$

Bartosiewicz et al. (2008) used both models in simulation of Kelvin–Helmholtz instability where surface tension forces are not dominant and the density ratio is small. Bartosiewicz et al. (2008) claimed that the results with different model for averaged factor do not differ significantly, but both models should be carefully assessed for large density ratios.

In the present paper, we consider the simulations with large density ratio and with surface tension force playing a dominant role. Several models for averaged factor were used: model based on volume and mass average, model where surface tension force is added only to momentum equation of liquid $\beta_1=1$ or gas phase $\beta_2=1$. The decision, which model is the most appropriate is presented in Section 3.1, where pressure jump over a droplet was analyzed.

2.2. Numerical discretization

To ensure divergence free velocity field, a pressure correction algorithm called SIMPLE (Semi-Implicit Method for Pressure-Linked Equations) is used to calculate pressure field (Ferziger and Perič, 1996). Here only a brief overview is given.

1. The momentum equation, without interfacial forces is solved to obtain intermediate velocity field of both phases $\vec{u}_1^*,\vec{u}_2^*$
2. The momentum equation is solved to get intermediate velocity field including interfacial forces $\vec{u}_1^*,\ \vec{u}_2^*$ with implicit treatment of drag force
3. The pressure correction equation is solved to assure mass conservation

$$\nabla\left(\frac{\nabla p'}{\rho_1}+\frac{\nabla p'}{\rho_2}\right)=-\frac{1}{\Delta t}\left(\nabla\cdot(\alpha_1\vec{u}_1^*)+\nabla\cdot(\alpha_2\vec{u}_2^*)\right) \tag{12}$$

4. Contribution of the pressure correction part is added to momentum equation to get new velocity field of both phases $\vec{u}_1^{n+1},\ \vec{u}_2^{n+1}$
5. The continuity equation for volume fraction is solved to obtain new volume fraction field α^{n+1}
6. Interface sharpening algorithm is applied
7. Finally the pressure correction is added to the old pressure

Eq. (12) is a Poisson equation and is solved with a stabilized conjugate gradient solver CGSTAB described in the book of Ferziger and Perič (1996). Equations are written in a discrete form using finite difference method. Staggered grid is used to avoid checkerboard distribution of the variables. Discretization of the convective part in Eqs. (1) and (2) is done with high resolution method, which combines upwind and Lax–Wendroff scheme with Van Leer flux limiter (LeVegue, 2002; Leskovar et al., 2006). The upwind scheme is used in the regions with large gradients and Lax–Wendroff scheme is used elsewhere. The high resolution method is between first and second-order accurate in space and results in great reduction of the numerical dissipation and diffusion.

The interfacial forces near the interface are usually large; that makes the system of equations stiff and requires special numerical treatment. Operator splitting method (Tiselj and Horvat, 2002) is used in the present work. In operator splitting method, the interfacial forces (stiff terms) are integrated with different, smaller timestep or calculated with implicit scheme as in our approach. System of two equations, with local velocities in each computational cell is solved in each iteration:

$$\frac{\alpha_1\rho_1(u_1^{n+1}-u_1^n)}{\Delta t}=(u_2^{n+1}-u_1^{n+1})\rho_m\alpha_1\alpha_2\frac{c_D}{d} \tag{13}$$

$$\frac{\alpha_2\rho_2(u_2^{n+1}-u_2^n)}{\Delta t}=(u_1^{n+1}-u_2^{n+1})\rho_m\alpha_1\alpha_2\frac{c_D}{d} \tag{14}$$

The system is analytically solved and the new velocities are calculated as:

$$u_1^{n+1}=\frac{u_1^n\left(1+\Delta t\frac{c_D}{d}\frac{\rho_m}{\rho_2}\alpha_1\right)+u_2^n\left(\Delta t\frac{c_D}{d}\frac{\rho_m}{\rho_1}\alpha_2\right)}{1+\Delta t\frac{c_D}{d}\frac{\rho_m}{\rho_1}\alpha_2+\Delta t\frac{c_D}{d}\frac{\rho_m}{\rho_2}\alpha_1} \tag{15}$$

$$u_2^{n+1}=\frac{u_1^n\left(\Delta t\frac{c_D}{d}\frac{\rho_m}{\rho_2}\alpha_1\right)+u_2^n\left(1+\Delta t\frac{c_D}{d}\frac{\rho_m}{\rho_1}\alpha_2\right)}{1+\Delta t\frac{c_D}{d}\frac{\rho_m}{\rho_1}\alpha_2+\Delta t\frac{c_D}{d}\frac{\rho_m}{\rho_2}\alpha_1} \tag{16}$$

The velocity of fluid 1 dominates where only fluid 1 is present if the inequality $\Delta t\frac{c_D}{d}\gg 1$ holds. In order to satisfy the inequality the interphase length scale is chosen as:

$$d=\frac{\Delta t c_D}{100} \tag{17}$$

Temporal discretization of the equations is explicit and first-order accurate. Two time constraints, which can be deduced from the discretized momentum Eq. (2) (Ferziger and Perič, 1996; Olsson and Kreiss, 2005) limit the timestep.

The convective time step limit (Courant) (18) is equal to the characteristic convection time, that is the time required for a disturbance to be convected over a distance of one cell

$$\Delta t_{convection}=\left(\left(\frac{\max(u)}{\Delta x}\right)^2+\left(\frac{\max(v)}{\Delta y}\right)^2\right)^{-1/2} \tag{18}$$

The mixture of upwind first-order and centered second-order approximations for the spatial derivates is used, where stability analysis considering only viscous terms requires the step size to be bounded by the viscous time limit (19). The viscous time limit is equal to the characteristic diffusion time, which is roughly the time required for a disturbance to be transmitted by diffusion over the cell.

$$\Delta t_{diffusion}=\frac{1}{4}\frac{\min(\rho_1/\mu_1,\rho_2/\mu_2)}{1/\Delta x^2+1/\Delta y^2} \tag{19}$$

In the code the minimum of both time constraints is used: $\Delta t\leqslant\min(\Delta t_{convection},\Delta t_{diffusion})$. In the pressure jump test case the most limiting is the viscous time step limit due to the small velocities. In oscillating bubble simulation the most limiting is the convective time step limit (Courant) at the beginning and viscous at the end (small velocities). The most limiting timestep in the simulation of rising bubble is the convective (Courant) time step limit.

2.3. Interface sharpening algorithm – implementation of wetting angle

In this section, conservative level set method Olsson and Kreiss (2005) used for interface sharpening is described. Free surface is smeared over several cells and even if we solve volume fraction advection Eq. (1) with the high resolution scheme the smearing is still increasing with time. The interface sharpening is indeed more

numerical than physical model. However we are using numerical (unphysical) model to eliminated another numerical artifact: the unphysical numerical diffusion of the interface. The overall result is in reasonable agreement with physics. Method consists of two steps. In the first step, the continuity equation for volume fraction (1) is solved with high resolution scheme. In the second step an equation that acts as an artificial compression, is solved:

$$\frac{\partial \alpha_1}{\partial \tau} + \nabla \cdot \left(\alpha_1 (1 - \alpha_1) \vec{n} \right) = \varepsilon \Delta \alpha_1 \tag{20}$$

In Eq. (20), $\vec{n}$ stands for the normal at the interface and is calculated only once in the beginning of the second step. We denote time variable by τ to stress that this is an artificial time, not equivalent to the actual time t. Artificial compression flux $\alpha_1(1-\alpha_1)\vec{n}$ acts in the regions where $0 < \alpha_1 < 1$ in the direction normal to the interface $\vec{n}$. The artificial compression flux eliminates the numerical diffusion of the volume fraction, which appears due to numerical discretization of convective part in advection equation for volume fraction (1). Small amount of "viscosity" ε is added to avoid discontinuities.

The value of "viscosity" ε is taken as low as possible to get the interface smeared over minimal number of cells

$$\varepsilon = \Delta x/2 \tag{21}$$

Too small ε compared to the grid size Δx results in over or undershoots of the volume fraction α. Since we use explicit time stepping we get stability restriction on $\Delta\tau$

$$\Delta\tau = \frac{\Delta x}{32} \tag{22}$$

As proposed by Olsson and Kreiss (2005) Eq. (20) is solved until the steady state is achieved. Nevertheless with the used artificial timestep (22) only one iteration is needed to significantly reduce the numerical diffusion.

The equation for normal at the wall boundary

$$\vec{n} = \vec{n}_{wall} \cos\theta + \vec{t}_{wall} \sin\theta \tag{23}$$

is proposed as a boundary condition for Eq. (20), even if no surface tension appears in the system (Štrubelj and Tiselj, submitted for publication). Eq. (23) summarizes the homogeneous Neumann boundary condition for α_1 (the spatial derivate of α_1 perpendicular to the wall) and adds boundary condition for spatial derivate of α_1 parallel to the wall. The wetting angle θ correlates interface normal to the wall normal $\vec{n}_{wall}$ and tangent $\vec{t}_{wall}$. The wetting angle θ in wetting and non-wetting systems is defined in Fig. 1.

The initial interface at $t = 0$ is smeared with the hyperbolic tangent function

$$\alpha_1 = (1 + \tanh((x - x_0)/\varepsilon))/2 \tag{24}$$

With the conservative level set method the free surface is still smeared through several cells (3–4 cells), as seen in Fig. 2, but the number of cells with smeared interface remains constant during the simulation and does not dependent on the number of cells used for discretization of the whole domain.

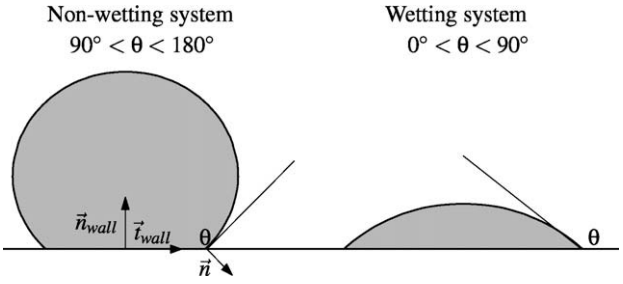

Fig. 1. Wetting and non-wetting system.

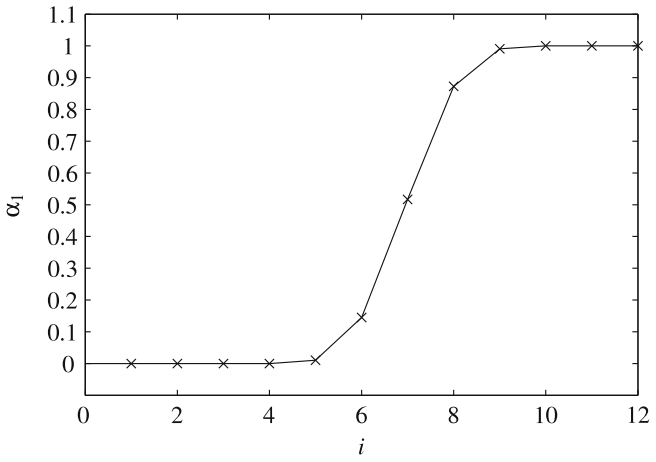

Fig. 2. Volume fraction α_1 smeared over several cells (i – cell number) using conservative level set method.

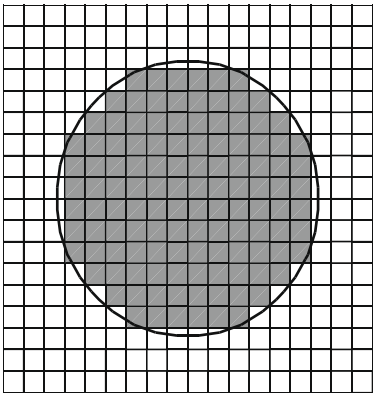

Fig. 3. Calculation of volume V_1 that is occupied by fluid 1 from volume fraction field α_1.

The advantage of conservative level set method is volume and mass conservation. The volume of fluid 1 is simply defined as the sum of all cell volumes where volume fraction is larger then 0.5, as presented in Fig. 3 and defined in Eq. (25). The volume calculation is quite robust, since interface is not reconstructed, but precise enough for comparison of volume conservation between different models

$$V_1 = \sum_{i,j} \begin{cases} 0; & \alpha_{1;i,j} > 0.5 \\ \Delta x \Delta y; & \alpha_{1;i,j} \leqslant 0.5 \end{cases} \tag{25}$$

3. Test cases

Four test cases were chosen to validate two-fluid model with interface sharpening and surface tension force. The first is a basic test case where pressure jump over a droplet interface is compared to analytical prediction and parasitic velocities are compared to the results of other interface tracking models based on single-fluid equations. The second is a test case where the oscillation time period of droplet is compared to the analytical one. The third is a test case where rising bubble terminal velocity and shape is analyzed and the fourth case includes two simulations of droplet on a horizontal wall with two wetting angles to demonstrate the implemented wetting angle.

3.1. Pressure jump over a droplet interface

The pressure jump over a droplet interface is proposed by Canot and Caltagirone (2004) as a test case for validating the proper implementation of surface tension. The pressure jump over the droplet interface and parasitic velocities are analyzed in simulation. Two-dimensional configuration is considered where an ethanol drop ($R = 2$ mm) is initially centered in a square cavity ($L = 7.5$ mm) full of air. A zero-gravity field is imposed, the flow is assumed to be isothermal and the surface tension is constant. The fluid properties are $\rho_1 = 787.88\ \mathrm{kg/m^3}$, $\mu_1 = 2.4 \cdot 10^{-2}$ Pa s for ethanol and $\rho_2 = 1.1768\ \mathrm{kg/m^3}$, $\mu_2 = 2 \cdot 10^{-3}$ Pa s for the air. The viscosity was increased by factor 20 comparing to the real viscosities in order to achieve higher dumping of spurious velocities and bubble shape oscillations 3.2) and faster stabilization of the bubble shape. The surface tension between the ethanol and air is $\sigma = 0.02361$ N/m. Initially, the velocity field is zero in the whole domain. Wall boundary conditions are considered in the problem.

Pressure jump over the interface due to surface tension in two dimensions is analytically calculated as:

$$\Delta p = \frac{\sigma}{R} \tag{26}$$

The pressure jump in analyzed two-dimensional system is 11.8050 Pa (26). The pressure field is smeared over the interface (Fig. 4), similar as the volume fraction. The pressure jump in simulations is overestimated for 15% (e) on a coarse grid (16×16) elements. The relative error ($\Delta p_{error} = 1 - \Delta p_{simulation}/\Delta p_{analytical}$) is decreasing with grid refinement (Fig. 5) with order of accuracy between 1.25 and 1.6, depending on the model for averaged factor β_k in (7). The minimum relative error (0.55%) and the best order of convergence ($H(\Delta x) = 1.6$) is obtained in the model for averaged factor β_k based on volume averaging (11) and in the model where surface tension force is added only to the gas momentum equation (Table 1). The pressure jump error in VOF simulations obtained by Canot and Caltagirone (2004) are from 2% to 0.5% and does not converge monotonically to the analytical value as the results of discussed two-fluid model.

The density ratio has no effect on the pressure jump error as shown in simulations with 32×32 cells (Table 2).

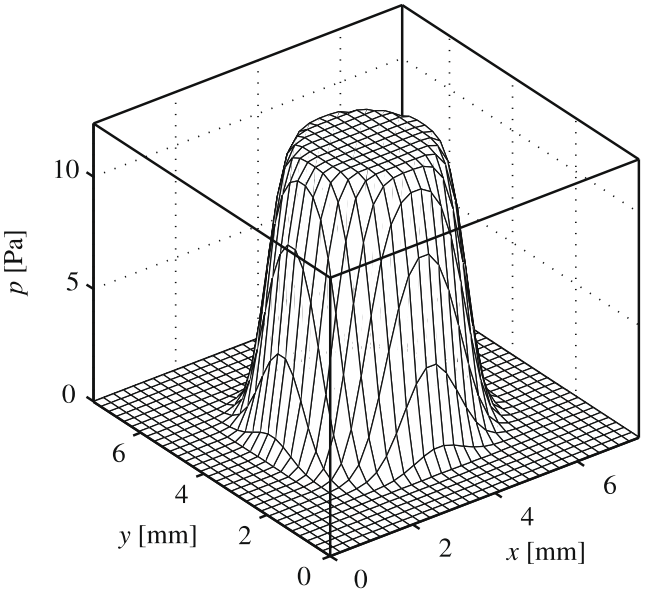

Fig. 4. Pressure field in simulation of the pressure.

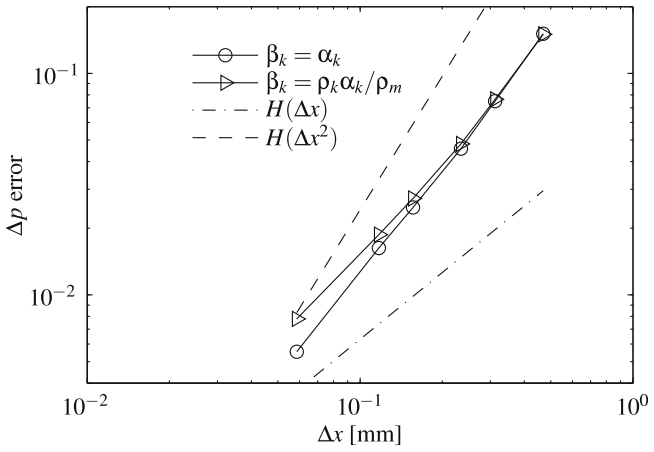

Fig. 5. Order of accuracy in pressure jump over droplet interface.

Table 1
Pressure jump over a droplet and numerically induced parasitic velocities in the ethanol in simulations with different models for averaged coefficients and calculated on 128×128 cells.

β_1	α_1	$\alpha_1\rho_1/\rho_m$	1	0	2
β_2	α_2	$\alpha_2\rho_2/\rho_m$	0	1	−1
$H(\Delta x)$	1.6807	1.5905	1.5852	1.6863	1.4825
Δp [Pa]	11.8704	11.8970	11.9080	11.8695	11.9467
Δp error [%]	0.55	0.78	0.87	0.55	1.20
C_p	$6.3 \cdot 10^{-4}$	$6.4 \cdot 10^{-4}$	$6.8 \cdot 10^{-4}$	$6.3 \cdot 10^{-4}$	$7.1 \cdot 10^{-4}$

Table 2
Pressure jump over a droplet in simulation with different density ratios, calculated on 32×32 cells.

ρ_1/ρ_2	1	10	100	1000
Δp [Pa]	12.3696	12.3686	12.3707	12.3752
Δp error [%]	4.78	4.77	4.79	4.83

Various numerical methods are known to generate spurious artificial numerical flows instead of keeping steady cylindrical drops (Canot and Caltagirone, 2004). The order of magnitude of parasitic velocities can be estimated according to the surface tension and dynamic viscosity of the drop:

$$u_p = \frac{C_p \sigma}{\mu_1} \tag{27}$$

where C_p is a numerical constant characteristic of the quality of the numerical modeling of surface tension forces (a non-dimensional number similar to a capillary number). The optimal value of C_p is zero. Typical values of C_p are found between 10^{-3} and 10^{-10}. We found the minimal parasitic velocities in simulations with averaged factor β_k based on volume averaging and model where surface tension force is added only to the gas momentum equation (Table 1). The minimum C_p in the analyzed two-fluid model is $6 \cdot 10^{-4}(5 \cdot 10^{-5})$ for VOF and $5 \cdot 10^{-7}$ for front-tracking (Canot and Caltagirone, 2004). The interface and the surface tension in conservative level set model are smeared over more cells then in VOF model; the result are higher parasitic velocities. Grid refinements has negligible effect on parasitic velocities.

The averaged factor model based on volume averaging (11) gives the best results and was used for all further simulations.

3.2. Oscillating droplet

Simulation of the oscillating droplet is the second part of the test case proposed by Canot and Caltagirone (2004). Two-dimen-

sional configuration is considered where an ethanol ellipsoidal drop ($r_{average} = 22.56$ mm) or square ($l = 40$ mm) is initially centered in a square cavity ($L = 75$ mm) full of air. A zero-gravity field is imposed, the flow is assumed to be isothermal and the surface tension is constant. Fluid properties are the same as in the previous test case. Initially, the velocity field is zero in the whole domain. The oscillation period in simulation of two-dimensional droplet with initially ellipsoid ($n = 2$) and square shape ($n = 4$) is compared to the approximate analytical solution:

$$\omega_0^2 = \frac{(n^3 - n)\sigma}{(\rho_1 + \rho_2)R^3} \tag{28}$$

$$\tau_0 = \frac{2\pi}{\omega_0} \tag{29}$$

where the ω_0 is oscillating frequency and τ_0 is oscillating time period.

The north pole interface position ($n = 2$ – Figs. 6 and 8, $n = 4$ – Figs. 7 and 9) is damped oscillation, where damping is larger on a coarse grid due to the larger numerical viscosity (discretization error in the convective part, which acts as a diffusive term) in the momentum equation.The oscillation time period is slightly changing with the grid refinement (Table 3), but remains in the range of ±5%. The oscillation time period for initially square droplet is smaller than for initially ellipsoid droplet. Almost constant interface position is observed in the simulation of initially square droplet after 6 s, but the parasitic velocities are still present. The constant interface thickness is observed from the volume fraction contours. The volume conservation is 1.5% on coarse grid and 0.15% on fine grid, respectively.

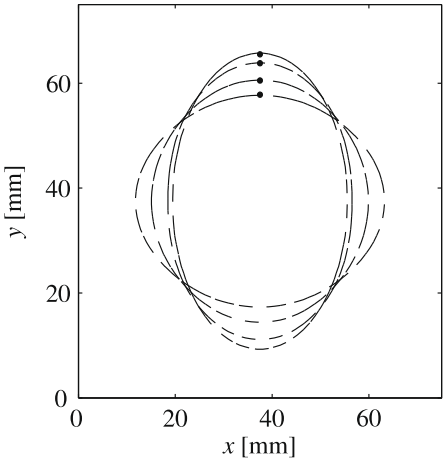

Fig. 6. Shape of the bubble in simulation of initially ($n = 2$) ellipsoidal droplet and the north pole interface position y at times t = 0.0, 0.2 0.4, 0.6 s.

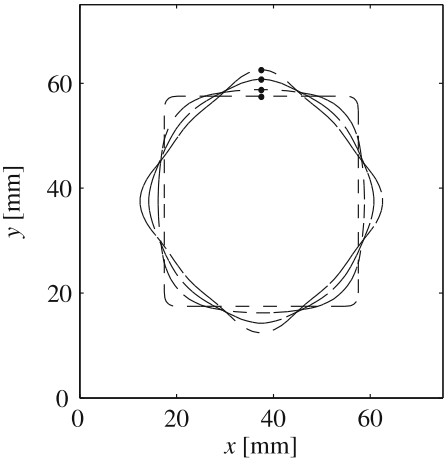

Fig. 7. Shape of the bubble in simulation of initially ($n = 4$) square droplet and the north pole interface position y at times t = 0.0, 0.2 0.4, 0.6 s.

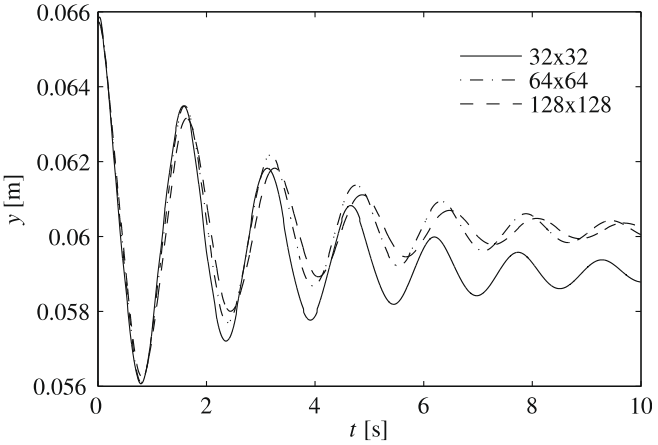

Fig. 8. North pole interface position y in simulation of initially ellipsoidal droplet on three different grids.

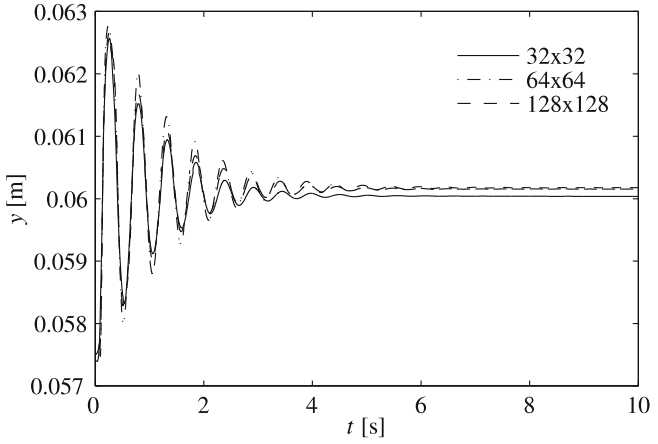

Fig. 9. North pole interface position y in simulation of initially square droplet on three different grids.

Table 3
Oscillation period of droplet in simulation with different numbers of cells.

Mode	Analytical	32 × 32	64 × 64	128 × 128
n = 2				
τ_0 [s]	1.5888	1.5582	1.5759	1.6150
τ_0 error [%]		−1.94	−0.81	1.6
n = 4				
τ_0 [s]	0.5024	0.5299	0.5164	0.5206
τ_0 error [%]		5.4	2.7	3.62

3.3. Rising bubble

The benchmark with rising bubble in a stagnant liquid was proposed by Hysing et al. (in press). Results of the two-fluid model with interface sharpening are compared with the results of the level set method. The gas bubble of density $\rho_2 = 100$ kg/m^3, viscosity $\mu_2 = 1$ Pa s and $R_0 = 25$ cm is rising in the liquid with

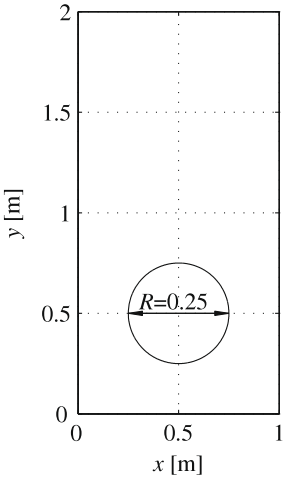

Fig. 10. Initial bubble position for test 3.3.

properties $\rho_1 = 1000\ \mathrm{kg/m^3}$ and $\mu_2 = 10\ \mathrm{Pa\,s}$. The chosen fluids are non-realistic and the purpose is to compare result obtained with different numerical models. The gravity in the system is $g = -0.98\ \mathrm{m/s^2}$ and the surface tension between fluids $\sigma = 24.5\ \mathrm{N/m}$. The corresponding dimensionless numbers are $Re = \rho_1\sqrt{g}(2R_0)^{3/2}/\mu_1 = 35$ and $Eo = 4\rho_1 g R_0^2/\sigma = 10$. Both fluids are at rest initially. The initial position of the bubble is shown in Fig. 10.

Several parameters were analyzed and compared to the result of Hysing et al. (in press): the position of bubble mass center vs. time, the rise velocity, volume of bubble and circularity C defined as the ratio of perimeter of area-equivalent circle and perimeter of a bubble P:

$$C = \frac{2\pi R_0}{P} \tag{30}$$

$$P = \int_V |\nabla\alpha| dV = \Delta x \Delta y \sum_{ij} \sqrt{\left(\frac{\alpha_{i+1j} - \alpha_{i-1j}}{2\Delta x}\right)^2 + \left(\frac{\alpha_{ij+1} - \alpha_{ij-1}}{2\Delta y}\right)^2} \tag{31}$$

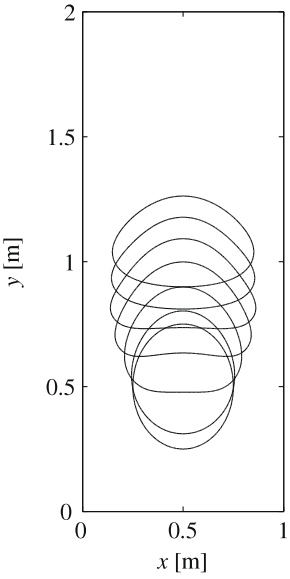

Fig. 11. Interface evolution of rising bubble at 0 s, 0.5 s, 1.0 s, 1.5 s, 2.0 s, 2.5 s and 3.0 s.

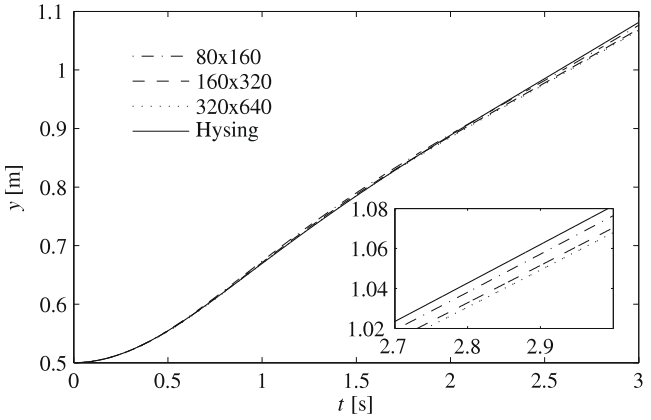

Fig. 12. Bubble mass center position y vs. time in simulation on different grids (320×640, 160×320 and 80×160 cells) and in simulation performed by Hysing et al. (in press).

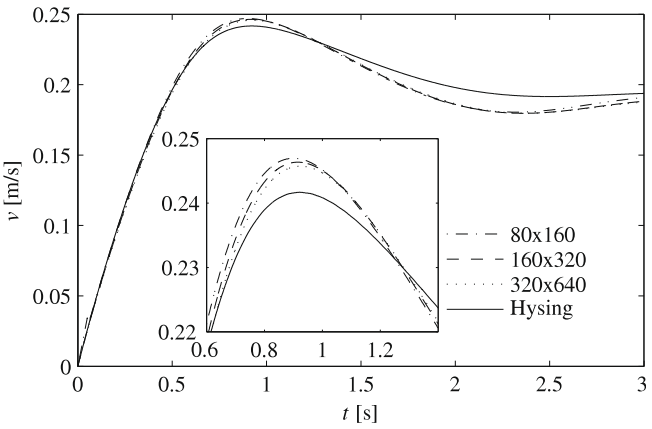

Fig. 13. Bubble rise velocity u_r in simulation on different grids (320×640, 160×320 and 80×160 cells) and in simulation performed by Hysing et al. (in press).

The circularity is obviously equal to 1 when the bubble is ideal circle and is reduced when the bubble is deformed.

The bubble shape development can be observed in Fig. 11. The position of center mass (Fig. 12) in simulation with analyzed two-fluid is 1.0679 m (1.0799–1.0817, Hysing et al., in press). The maximum velocity (Fig. 13) is 0.2457 m/s (0.2417–0.2421, Hysing et al.,

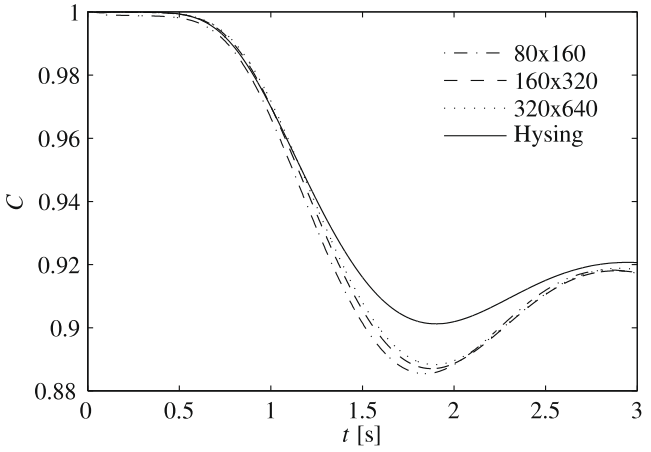

Fig. 14. Bubble circularity C in simulation on different grids (320×640, 160×320 and 80×160 cells) and in simulation performed by Hysing et al. (in press).

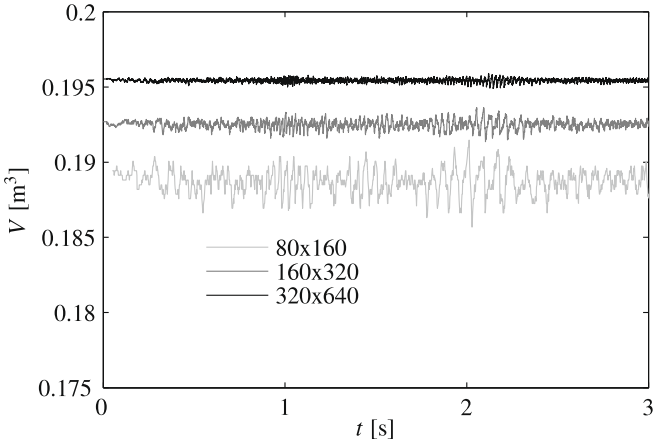

Fig. 15. Bubble volume V in simulation on different grids (320×640 cells – upper, 160×320 cells – middle and 80×160 cells – bottom curve).

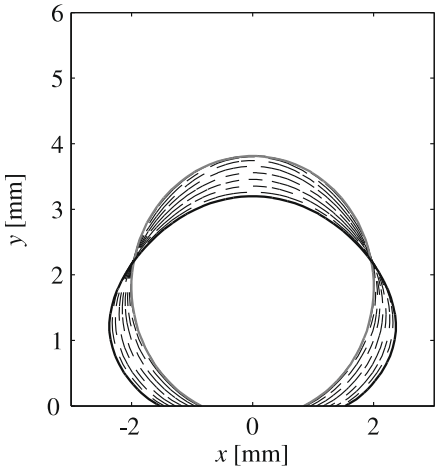

Fig. 17. Droplet on a surface with wetting angle $\theta = 255^\circ$.

in press) at time 0.9235 s (0.9214–0.9214, Hysing et al., in press). The minimum circularity (Fig. 14) is 0.8876 (0.9011–0.9013, Hysing et al., in press) at time 1.8915 s (1.875–1.9041, Hysing et al., in press). The bubble volume conservation is between 0.4% on the coarse grid and 0.05% on the fine grid (Fig. 15). To summarize: the results of the two-fluid model are very similar to the results of the level set (Hysing et al., in press) and deviate only up to 1.6%.

3.4. Wetting angle

Different wetting angles can be taken into account within the analyzed two-fluid model with interface sharpening and surface tension. Droplet of water at rest on a horizontal wall in the air is used for demonstration. The initial droplet is flattened due to the gravity $g = -9.81\ \mathrm{m/s^2}$), the flow is assumed to be isothermal and the surface tension is constant. The fluid properties are $\rho_1 = 1000\ \mathrm{kg/m^3}$, $\mu_1 = 1\ \mathrm{Pa\ s}$ (instead of using real value of 10^{-3} Pa s, a higher value was used to dump the bubble shape oscillations) for water and $\rho_2 = 1.1768\ \mathrm{kg/m^3}$, $\mu_2 = 10^{-5}\ \mathrm{Pa\ s}$ for air. The surface tension between the water and air is $\sigma = 0.073$ N/m.

The wetting angle is implemented in the two-fluid model with interface sharpening in such a way that the interface normal to the wall is calculated from (23). This normal is needed in the interface sharpening algorithm (20) and for calculation of interface curvature (6) in the cell near the wall. Dimension of the closed box in Figs. 16 and 17 is 6×6 mm and the box is discretized with 64×64 cells. The initial droplet shape corresponds to the cut off circular droplet with prescribed wetting angle. The droplet reaches the final shape due to the gravity. The wetting angle remains constant during the transient, since it is implemented as a boundary condition.

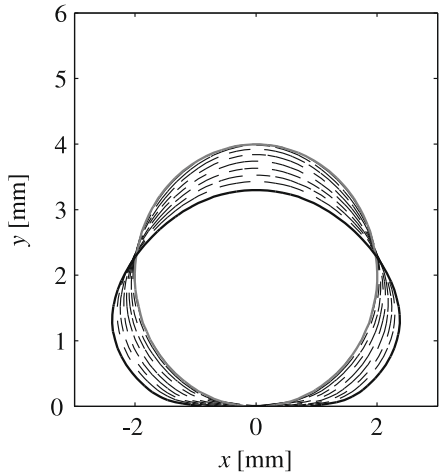

Fig. 16. Droplet on a surface with wetting angle $\theta = 5^\circ$.

4. Conclusions

The two-fluid model with interface sharpening and surface tension for simulation of free surface flows is presented. The surface tension force model is validated on several test cases where surface tension force is one of the dominating forces in the system and the density ratio is large. The surface tension force splitting between the two phases is described and multiple models are tested. We have shown that all models for averaged factors give more or less similar pressure jump over the droplet interface on the coarse grid. With grid refinement the results with volume averaged factor and model where surface tension is implemented only in gas momentum equation (momentum equation of the phase with lower density) give minimum error in pressure jump. The parasitic velocities in the simulation are one order of magnitude larger than in the simulations with VOF. The droplet oscillating time periods are very similar to the analytical prediction. In the simulation of the rising bubble the position, velocity, circularity and volume conservation of the bubble are comparable to the results obtained with other models. The wetting angle is also implemented in the case where the droplet shape on the horizontal wall with different wetting angles is simulated.

The short-term goal is to verify the two-fluid model with interface sharpening and surface tension with experiments. Our long-term goal is to improve quality of the simulations of the mixed two-phase flows, which are characterized by the dispersed and stratified flows being present in the same computational domain. In the subdomain filled with the dispersed phase the interface will not be sharpened, but modeled with the original (dispersed) two-fluid model and force models between phases developed for dispersed flows. The surface in the region with stratified flow will be sharpened with possible implementation of the surface tension force. Beside the interface sharpening model implemented within the two-fluid model and described in the present work, another, probably even more important sub-model is needed for such simulations: a criteria that determines whether the flow is closer to dispersed or stratified form, i.e., whether to switch on or off the interface tracking algorithm. The criteria for transition between stratified and dispersed flow is believed to be very important as it presents some kind of a basic “flow regime map” for the 3D

two-fluid model. The basic "flow regime map" should distinguish between sub-grid interface structures and interfaces with characteristic length scale larger than the grid spacing. A simple transition model proposed by Černe et al. (2001) was successfully implemented within our two-fluid model with interface tracking, and improvement of this model remains in the focus of our work.

Acknowledgements

The work was financially supported by the Slovene Ministry of Higher Education, Science and Technology through young researcher project 3311-04-831075 and NURISP project of the seventh framework program of EU.

References

ANSYS, 2007. CFX-11 Documentation. Solver Theory, Multiphase Flow Theory, ANSYS.

Bartosiewicz, Y., Laviéville, J., Seynhaeve, J.M., 2008. A first assessment of the NEPTUNE_CFD code: instabilities in a stratified flow comparison between the VOF method and a two-field approach. International Journal of Heat and Fluid Flow 29 (2), 460–478.

Bestion, D., 1990. The physical closure laws in the CATHARE code. Nuclear Engineering and Design 124 (3), 229–245.

Brackbill, J.U., 1992. A continuum method for modeling surface tension. Journal of Computational Physics 100 (2), 335–354.

Canot, E., Caltagirone, J.-P., 2004. Test-case no. 10: parasitic currents induced by surface tension (PC). Multiphase Science and Technology 16, 69–74.

Černe, G., 2001. Two-fluid simulation with the coupling of volume-of-fluid model and two-fluid model. Ph.D. Thesis, University in Ljubljana, Slovenia.

Černe, G., Petelin, S., Tiselj, I., 2001. Coupling of the interface tracking and the two-fluid models for the simulation of incompressible two-phase flow. Journal of Computational Physics 171 (2), 776–804.

Černe, G., Petelin, S., Tiselj, I., 2002. Numerical errors of the volume-of-fluid interface tracking algorithm. International Journal for Numerical Methods in Fluids 38, 329–350.

Coste, P., Pouvreau, J., Morel, C., Laviéville, J., Boucker, M., Martin, A., 2007. Modeling turbulence and friction around a large interface in a three-dimension two-velocity Eulerian code. In: 12th International Topical Meeting on Nuclear Reactor Thermal Hydraulics, NURETH-12. Pittsburgh, PA, USA.

Coste, P., Pouvreau, J., Laviéville, J., Boucke, M., 2008. A two-phase cfd approach to the pts problem evaluated on COSI experiment. In: Proceedings of the 16th International Conference on Nuclear Engineering. Orlando, FL, USA.

Crowe, C.T., 2005. Multiphase Flow Handbook. CRC Press.

Ferziger, J., Perič, M., 1996. Computational Methods for Fluid Dynamics. Springer-Verlag.

Frank, T., 2005. Numerical simulation of slug flow regime for an air–water two-phase flow in horizontal pipes. In: The 11th International Topical Meeting on Nuclear Reactor Thermal-Hydraulics (NURETH-11). Avignon, France.

Harlow, F.H., Welch, J.E., 1965. Numerical calculation of time-dependent viscous incompressible flow of fluid with free surface. Physics of Fluids 8 (12), 2182–2189.

Hirt, C.W., Nichols, B.D., 1981. Volume of fluid (VOF) method for the dynamics of free boundaries. Journal of Computational Physics 39 (1), 201–225.

Hirt, C.W., Amsden, A.A., Cook, J.L., 1974. An arbitrary Lagrangian–Eulerian computing method for all flow speeds. Journal of Computational Physics 14 (3), 227–253.

Höhne, T., Valleé, C., Prasser, H.-M., 2007. Experimental and numerical prediction of horizontal stratified flows. In: ICMF 2007 International Conference on Multiphase Flow on Multiphase Flow. Leipzig, Germany.

Hyman, J.M., 1984. Numerical methods for tracking interfaces. Physica D: Nonlinear Phenomena 12 (1–3), 396–407.

Hysing, S., Turek, S., Kuzmin, D., Parolini, N., Burman, E., Ganesan, S., Tobiska, L., in press. Quantitative benchmark computations of two-dimensional bubble dynamics. International Journal for Numerical Methods in Fluids, doi:10.1002/fld.1934.

Ishii, M., Hibiki, T., 2006. Thermo-Fluid Dynamics of Two-Phase Flow. Springer-Verlag.

Končar, B., Krepper, E., 2008. CFD simulation of convective flow boiling of refrigerant in a vertical annulus. Nuclear Engineering and Design 238 (3), 693–706.

Leskovar, M., Končar, B., Cizelj, L., 2006. Simulation of a reactor cavity steam explosion with a general purpose computaional fluid dynamics code. Strojniški Vestnik. Journal of Mechanical Engineering 52 (5), 292–308.

LeVegue, R., 2002. Finite Volume Methods for Hyperbolic Problems. Cambridge University Press.

Minato, A., Takamori, K., Ishida, N., 2000. An extended two-fluid model for interface behaviour in gas–liquid two-phase model. In: Proceedings of ICONE8. Baltimore, USA.

Nagayoshi, T., Minato, A., Misawa, M., Suzuki, A., Kuroda, M., Ichikawa, N., 2003. Simulation of multi-dimensional heterogeneous and intermittent two-phase flow by using an extended two-fluid model. Journal of Nuclear Science and Technology 40 (10), 827–833.

Olsson, E., Kreiss, G., 2005. A conservative level set method for two phase flow. Journal of Computational Physics 210 (1), 225–246.

Osher, S., Sethian, J.A., 1988. Fronts propagating with curvature-dependent speed: algorithms based on Hamilton–Jacobi formulations. Journal of Computational Physics 79 (1), 12–49.

Prasser, H.M., Ezsol, G., Baranyai, G., 2004. PMK-2 water hammer tests, condensation caused by cold water injection into main steam-line of VVER-440-type PWR – quick-look report (QLR). Tech. Rep., WAHALoads project deliverable D48.

Scheuerer, M., Galassi, M.C., Coste, P., D'Auria, F., 2007. Numerical simulation of free surface flows with heat and mass transfer. In: 12th International Topical Meeting on Nuclear Reactor Thermal Hydraulics, NURETH-12. Pittsburgh, PA, USA.

Štrubelj, L., Tiselj, I., submitted for publication. Interface sharpening in simulations with two-fluid model. International Journal for Numerical Methods in Engineering.

Sussman, M., 1994. A level set approach for computing solutions to incompressible two-phase flow. Journal of Computational Physics 114 (1), 146–159.

The RELAP5 Code Development Team, 1995. Relap5/MOD3 Code Manual Models and correlations. Idaho Falls.

Tiselj, I., Horvat, A., 2002. Accuracy of the operator splitting technique for two-phase flow with stiff source terms. In: Proceedings of the 2002 ASME Joint US–European Fluids Engineering Conference, vol. 257. Montreal, Que, Canada, pp. 1165–1171.

Tiselj, I., Černe, G., Horvat, A., Gale, J., Parzer, I., Giot, M., Seynhaeve, J.M., Kucienska, B., Lemonnier, H., 2004. WAHA3 code manual. Tech. Rep., WAHALoads project deliverable D10. <http://www2.ijs.si/r4www/IT/waha3_manual.pdf>.

Tryggvason, G., Bunner, B., Esmaeeli, A., Juric, D., Al-Rawahi, N., Tauber, W., Han, J.S.N., Jan, Y., 2001. A front-tracking method for the computations of multiphase flow. Journal of Computational Physics 169 (2), 708–759.

Vallée, C., Höhne, T., Prasser, H.-M., Sühnel, T., 2005. Experimental modelling and CFD simulation of air/water flow in a horizontal channel. In: The 11th International Topical Meeting on Nuclear Reactor Thermal-Hydraulics (NURETH-11). Avignon, France.

Wintterle, T., Laurien, E., Stäbler, T., Meyer, L., Schulenberg, T., 2008. Experimental and numerical investigation of counter-current stratified flows in horizontal channels. Nuclear Engineering and Design 238 (3), 627–636.

Yao, W., Bestion, D., Coste, P., Boucker, M., 2005. A three-dimensional two-fluid modeling of stratified flow with condensation for pressurized thermal shock investigations. Nuclear Technology 152 (1), 129–142.